

NACA RM E55F30

NACA

## RESEARCH MEMORANDUM

A VARIABLE-GEOMETRY AXISYMMETRIC SUPERSONIC

INLET WITH TELESCOPING CENTERBODY

By James F. Connors and Rudolph C. Meyer

Lewis Flight Propulsion Laboratory  
Cleveland, Ohio

CLASSIFICATION CHANGED

To UNCLASSIFIED

By authority of

*NACA Res also**1 RN-128*

Date

*effective*  
*Jan 24, 1958**AMT 9-9-58*

CLASSIFIED DOCUMENT

This material contains information affecting the National Defense of the United States within the meaning of the espionage laws, Title 18, U.S.C., Secs. 793 and 794, the transmission or revelation of which in any manner to an unauthorized person is prohibited by law.

NATIONAL ADVISORY COMMITTEE  
FOR AERONAUTICS

WASHINGTON

September 7, 1955

~~CONFIDENTIAL~~

## NATIONAL ADVISORY COMMITTEE FOR AERONAUTICS

RESEARCH MEMORANDUM

## A VARIABLE-GEOMETRY AXISYMMETRIC SUPERSONIC

## INLET WITH TELESCOPING CENTERBODY

By James F. Connors and Rudolph C. Meyer

## SUMMARY

For achieving good supersonic inlet performance over a wide range of Mach number, an axisymmetric variable-geometry technique has been proposed and demonstrated. A centerbody consisting of a number of individual, translating, concentric elements was used to produce a discontinuous surface, the envelope of which approximated any desired contour. Several stepped-spike configurations were studied at Mach number 3.85 and appraised on the basis of schlieren observations and pressure surveys of the resulting compression fields. Experimentally, it was observed that local elements of boundary-layer separation occurred ahead of each surface discontinuity and produced an effective bridging for the main flow.

An inlet with such a telescoping spike was designed and experimentally evaluated. Maximum total-pressure recoveries of 0.60 and 0.89 were realized at Mach numbers of 3.05 and 1.90, respectively. At both Mach numbers, supercritical mass-flow ratios near unity were obtained with subcritical stability ranges of 21 and 38 percent of maximum possible capture mass flow. The losses incurred as a result of surface discontinuities amounted to total-pressure-recovery decrements of 0.04 and 0.03 at free-stream Mach numbers of 3.05 and 1.90, respectively, when compared with that obtained with equivalent smooth-contour centerbodies. Increases in angle of attack generally produced moderate decreases in both recovery and mass flow.

## INTRODUCTION

For application to jet aircraft operating over a wide range of supersonic Mach number, the air induction system must incorporate some degree of flexibility in order to maintain a high level of efficiency. Consideration must be given such design variables as the degree of compressive flow turning (surface angle), flow detachment factors (cowl-lip angles), internal-area contraction (ducting), and initial-shock-angle

variation (cowl-position parameter). The attainment of high performance throughout the speed range requires, in general, that the inlet design be somewhat compromised and include variable-geometry features. Compared with the two-dimensional inlets which can use axial ramp translation or variation of the compression-surface angles, or both, the axisymmetric inlets present a more complex problem for variable Mach number operation.

Current axisymmetric technique is simply one of spike translation (ref. 1). For Mach numbers up to approximately 2.0 or for a very limited speed range, this method appears adequate. However, for operation to considerably higher Mach numbers, this technique which utilizes a fixed spike contour results in steep-angle cowls and large cowl projected areas, largely because of the necessity of avoiding internal contraction. For high variable Mach number operation, then, there is a definite need for improved axisymmetric variable-geometry technique for supersonic inlets.

The investigation reported herein was conducted at the NACA Lewis laboratory to explore the possibilities of effecting a spike contour variation in addition to axial translation. The proposed method schematically illustrated in figure 1 is to use a number of individual elements that can translate relative to one another as in a telescoping arrangement and produce a discontinuous surface. The envelope of this surface coincides with the desired contour as in figure 1(b). Aerodynamic considerations suggest that the boundary layer would separate ahead of each surface discontinuity, or step, and produce an effective bridging for the main flow. The use of a conical separation element for a proposed inlet application is successfully demonstrated in reference 2. From a structural viewpoint, of course, the complexity of such a telescoping spike depends upon the number of elements, and some arrangement must be made for scheduling their relative positions with flight Mach number.

The present study is specifically directed toward evaluating the pressure losses incurred as a result of centerbody surface discontinuities and determining the performance of a simulated axisymmetric variable-geometry inlet. At Mach number 3.85, surveys were made of the flow over spikes with surface bumps and compared with that over a smooth spike. At Mach numbers of 3.05 and 1.90, the performance of a simulated telescoping inlet was evaluated in terms of pressure recovery and mass-flow ratio. Angle-of-attack effects were also determined.

## SYMBOLS

The following symbols are used in this report:

- M Mach number  
m mass flow, slugs/sec  
P total pressure, lb/sq ft  
R duct radius at diffuser exit, ft  
r local tube radius, ft  
 $\alpha$  angle of attack, deg

## Subscripts:

- l local pitot  
0 free stream  
3 diffuser exit

## APPARATUS AND PROCEDURE

The experimental program was conducted essentially in two parts; the first was a preliminary survey study of the flow over several spikes with various surface discontinuities at Mach number 3.85, and the second was a performance evaluation of a simulated variable-geometry axisymmetric inlet with telescoping centerbody at Mach numbers 3.05 and 1.90.

## Spike Survey Study

Probe surveys of the flow over various spikes were made at a Mach number of 3.85 in the Lewis 2- by 2-foot wind tunnel. The air was maintained at a stagnation temperature of  $200^{\circ} \pm 5^{\circ}$  F and at a dew-point temperature of  $-20^{\circ} \pm 5^{\circ}$  F. In the test chamber, the Reynolds number per foot was approximately  $1.03 \times 10^6$  and the simulated pressure altitude was 108,000 feet.

The survey-spike configurations are illustrated in the photographs of figure 2. Coordinate dimensions are given in table I. The smooth-contour spike (the same as that used in ref. 3) was designed for focused compression by the method of characteristics. Except for the initial conical shock loss (0.99 total-pressure recovery), the flow along the

spike was to be compressed isentropically down to a Mach number of 2.45. As shown in figure 2, discontinuous spike contours were fabricated with step elements having leading-edge angles of  $90^\circ$  and  $30^\circ$ . The envelope contours of these spikes were identical to that of the smooth-contour spike.

As in the procedure of reference 3, a pitot probe traversed the flow field in a radial line from the axis of symmetry and passed through the main shock intersection as determined from schlieren observations. The probe tip was aligned parallel to the spike surface and was actuated by a motor and screw arrangement. An electric contact indicator was used to determine a zero reference position. As measured by a static tap on the spike surface at the survey station, the static pressure was assumed constant through the flow field out to the shock. This static pressure and the probe pitot pressures were used to calculate the local stream Mach numbers.

#### Variable-Geometry-Inlet Study

The inlet experiments were conducted in two different facilities in order to obtain the desired Mach numbers. Tests were run at a Mach number of 1.90 and a simulated pressure altitude of 45,000 feet in the Lewis 18- by 18-inch wind tunnel. The air was maintained at a stagnation temperature of  $150^\circ \pm 5^\circ$  F and at a dew-point temperature of  $-30^\circ \pm 5^\circ$  F. Based on the 2.90-inch inlet capture diameter, the Reynolds number was  $0.78 \times 10^6$ . The Mach 3.05 tests were run in another Lewis 18- by 18-inch wind tunnel. The test conditions were as follows: stagnation temperature,  $150^\circ \pm 5^\circ$  F; dew-point temperature,  $-20^\circ \pm 5^\circ$  F; Reynolds number,  $0.44 \times 10^6$ ; and simulated pressure altitude, 82,000 feet.

As shown in the schematic drawing of figure 3(a), the diffuser model was strut-mounted from the tunnel wall. A movable exit plug was used to regulate the inlet back pressure. In the support assembly, provisions were incorporated to permit angle-of-attack variation. A twin-mirror schlieren system was used to observe the inlet air-flow patterns.

The experimental version of the axisymmetric variable-geometry inlet with telescoping spike is illustrated in the schematic drawing of figure 3(b) and the photograph of figure 3(c). For this investigation, solid spikes with the discontinuities cut into them were used to simulate the telescoping geometry. Coordinate dimensions of the cowl and the two spikes are given in table II. The inlet was designed to capture the maximum possible free streamtube of air and to maintain attached shocks on the cowl at Mach numbers of 1.90 and 3.05. The centerbody envelope contours were designed for focused compression at

the cowl lip by the method of characteristics. Existing characteristics solutions (for spikes of refs. 4 and 5) were used with the consequence of having the different initial cone angles of  $40^\circ$  for the Mach 1.90 spike and  $30^\circ$  for the Mach 3.05 spike. Actually, in order to reduce the number of elements, it would have been desirable to have had the same initial angle for tests of such a variable-geometry inlet application. The theoretical final Mach number at the diffuser entrance was approximately 1.26 and 1.76 at free-stream Mach numbers of 1.90 and 3.05, respectively. Eight translating concentric elements were rather arbitrarily selected to make up the centerbody. For each element, the upstream face contour was determined by the steepest-angle required at either end of the Mach number range. Thus, the face contours of the initial elements were determined by the Mach 1.90 envelope contour with its greater initial angle and the rearward elements by the Mach 3.05 envelope contour with its greater surface flow-turning angles. The resulting configuration (figs. 3(b) and (c)) then consisted of a spike at Mach 3.05 with moderately small surface discontinuities near the tip, but otherwise a smooth contour back into the diffuser. At Mach 1.90, the spike telescoped into a smooth external compression surface up to the entrance, but with rather abrupt surface discontinuities on the turn or shoulder.

Two other spikes were fabricated in order to establish a basis for comparison. These were the smooth-contour geometries which the telescoping spike was designed to approximate. The contours of these spikes were then identical to the envelope contours of the telescoping arrangement.

The internal-duct area variations based on the envelope contours are presented in figure 3(d). Downstream of the common point, the area distribution conformed approximately to an equivalent  $5^\circ$  conical area expansion. Initially the Mach 1.90 spike had a constant-area section that corresponded to the turning of the flow back to the axial direction. In contrast to this, the Mach 3.05 contour had initially fairly rapid area divergence to the common point and a very slight internal contraction.

At the diffuser exit were located a 21-tube total-pressure rake and 4 wall static-pressure orifices. Total-pressure recovery was obtained by an area-weighted integration. Mass flow was based on the measured static pressure at the rake station and the sonic discharge area at the plug with the assumption of isentropic one-dimensional flow between the two stations. A calibration of this measuring technique was obtained from data with an inlet capturing a known free streamtube of air.

## RESULTS AND DISCUSSION

## Spike Survey Study

The air-flow patterns obtained with the stepped spikes are shown in figure 4. With the  $90^\circ$  stepped spike, the first several steps were neatly bridged by individual elements of boundary-layer separation. The rearward steps, however, were submerged in the boundary layer with separation appearing to extend over the steps with some unsteadiness in the local flow. In general, the over-all pattern showed the flow following, at least approximately, along the envelope contour of the spike.

With  $30^\circ$  angles on the face of each step, the configuration represented a spike which could be telescoped back into a single-shock,  $30^\circ$  half-angle cone, such as would be suitable as a centerbody at a free-stream Mach number of 2.0. The resultant pattern (fig. 4(b)) appeared considerably different from that of the  $90^\circ$  stepped spike. Schlieren observations indicated that the flow was quite steady with bridging occurring across each step as a result of local boundary-layer separations. In some of the rearward steps, the amount of separation might even be somewhat inadequate because the flow seemed to overexpand at the shoulders and thus produce stronger shocks (and correspondingly higher losses) than if the separation had completely filled the surface discontinuity. From these observations, it was concluded that, because of the generally satisfactory over-all compression envelope and shock coalescence, such a telescoping arrangement might find application as a supersonic inlet centerbody.

In order to determine the total-pressure losses associated with such surfaces, a pitot-probe survey was made for each of three contours. The survey line was a radial line from the axis of symmetry passing through the main shock intersection.

The results of these pressure surveys are presented in figure 5. A considerably thicker boundary layer was encountered near the surface of the stepped spikes when compared with the results for the smooth-contour spike (ref. 3). Outside this boundary layer, the survey-plane Mach numbers checked roughly with the theoretical design value. An area-weighted integration of the pitot-pressure distribution was used to obtain an inlet recovery potential for each configuration. This value would thus include the normal shock loss. Compared with the result for the smooth-contour spike (0.47), the  $30^\circ$  stepped spike value (0.40) indicated a 15-percent decrease in potential recovery as a result of the irregular surface; but the  $90^\circ$  stepped spike value (0.37) indicated a 21 percent decrease. It may also be noted that, largely because of the displacement effect of the larger boundary layers, the main shock intersection was located farther out from the surface of the stepped spike than was that for the smooth spike.

These preliminary results with abruptly stepped spike configurations were considered quite satisfactory with respect to applying this technique to an actual inlet problem, for which fewer and less-severe step geometries might be suitable. Accordingly, a simulated variable-geometry inlet was designed and studied at Mach numbers of 3.05 and 1.90.

#### Variable-Geometry-Inlet Study

Diffuser performance characteristics are presented in figure 6. At zero angle of attack this variable-geometry inlet with a telescoping centerbody yielded at Mach number 1.90 a maximum total-pressure recovery of 0.89, a critical recovery of 0.88, and a maximum mass-flow ratio of 0.98. Stable subcritical operation was obtained down to a mass-flow ratio of 0.60. Compared with the ideal smooth-contour design, which gave a maximum recovery of 0.92, the model with internal surface discontinuities resulted in a total-pressure-recovery decrement of 0.03. At a free-stream Mach number of 3.05, a critical pressure recovery of 0.57 was obtained at a mass-flow ratio of 0.99. The maximum recovery of 0.60 was realized at a minimum stable mass-flow ratio of 0.79. When compared with the performance of the smooth-contour design (maximum recovery = 0.61), a total-pressure-recovery decrement of 0.04 was chargeable to the external surface discontinuities. At Mach number 3.05, the irregular compression surface resulted in a much greater stable subcritical operating range than was realized with its smooth counterpart.

Angle-of-attack performance of the variable-geometry inlet is presented in figure 6 and summarized in the cross plot of figure 7. In general, increased angle of attack caused reductions in critical recovery, supercritical mass-flow ratio, and stable subcritical operating range. At a Mach number of 3.05 and an angle of attack of  $6^\circ$ , extensive separation off the top or lee side of the spike was encountered at mass flows less than the minimum stable value. This was a steady pattern; however, the associated discontinuity in the performance curve at the minimum stable value was quite pronounced.

Zero-angle-of-attack flow patterns for the variable-geometry inlet are shown by the schlieren photographs of figure 8. At Mach number 3.05, boundary-layer separation was observed to bridge the external surface discontinuities on the spike. A slight shock detachment at the cowl lip occurred during supercritical operation. At the minimum stable mass-flow condition, the diffuser shock was located out on the spike forward of the cowl lip. At Mach number 1.90 (fig. 8(b)) the observed flow patterns were the same as that observed with the smooth on-design inlet configurations of reference 4. As the diffuser shock moved out on the spike, the entire flow was quite stable with the boundary layer downstream of

the bow shock appearing to be attached to the surface and to follow the contour back into the inlet. This lack of separation was a favorable consequence of the low surface Mach number of 1.20 at the diffuser entrance. With an increase in back pressure and coincident with the onset of inlet buzz, the boundary layer was observed to lift and separate from the spike because of increased shock strength due to a higher compression-surface Mach number. This separation presumably choked the inlet and triggered the buzz cycle.

Air-flow patterns obtained with the variable-geometry inlet at various angles of attack are also included in figure 8. At Mach number 3.05, body cross-flow effects caused some thickening of the boundary layer on the top or lee side of the spike with increasing angle of attack. At an angle of attack of  $6^\circ$  and mass flows less than the minimum stable value with attached flow, large-scale separation (fig. 8(e)) extended forward to the spike tip. The boundaries of this steady separation pattern tended to take the form of a cone aligned in the free-stream direction. Coincident with this change in subcritical flow pattern was a large discontinuity in mass flow into the inlet. Photographs of the shock patterns at a Mach number of 1.90 for angles of attack of  $4^\circ$  and  $8^\circ$  are shown in figures 8(d) and (f), respectively. These patterns are again practically the same as those observed for the on-design fixed-geometry inlets of reference 4.

Total-pressure profiles across the diffuser exit during critical inlet operation are shown in figure 9. These profiles were, no doubt, favorably influenced by the approximately 2 diameters of constant-area mixing length between the diffuser exit and the rake station. At a free-stream Mach number of 1.90, the wake off the centerbody caused a dip in the zero-angle-of-attack profile. At Mach number 3.05, the profiles were quite flat and uniform at zero angle of attack. These differences in total-pressure distributions were also influenced by the difference in diffuser-exit Mach number (at  $M_0 = 3.05$ ,  $M_3 = 0.15$ ; at  $M_0 = 1.90$ ,  $M_3 = 0.28$ ). With increasing angle of attack there was a tendency at both Mach numbers toward separation in the lower quadrant.

#### CONCLUDING REMARKS

For application to jet aircraft operating over a wide range of supersonic Mach number, an axisymmetric nose inlet with telescoping centerbody has been proposed. Herein, preliminary experimental studies have demonstrated the feasibility of using boundary-layer separation to accommodate the flow over steps or surface discontinuities resulting from telescoping spike configurations. Such an inlet was designed and found to yield maximum total-pressure recoveries of 0.89 at a Mach number of

1.90 and 0.60 at a Mach number of 3.05. At both Mach numbers, supercritical mass-flow ratios near unity were obtained with subcritical stability ranges of 38 and 21 percent of maximum possible mass flow. Compared with data for the smooth-contour geometry, the flow losses, which were incurred as a result of surface discontinuities, amounted to total-pressure-recovery decrements of 0.03 and 0.04 at free-stream Mach numbers of 1.90 and 3.05, respectively.

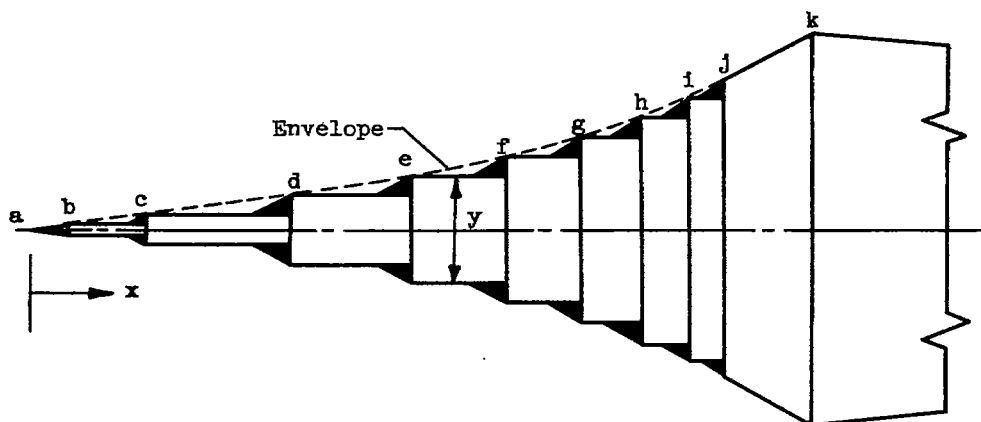
Possibilities of lessening the degree of complexity without penalizing performance lie in the direction of reducing the number of translating elements. For the configuration studied, this could have been accomplished by the choice of the same initial cone angle for each Mach number. Accordingly, minimizing the number of elements and optimizing the location and design of these elements would require further research.

Lewis Flight Propulsion Laboratory  
National Advisory Committee for Aeronautics  
Cleveland, Ohio, July 5, 1955

#### REFERENCES

1. Gorton, Gerald C.: Investigation at Supersonic Speeds of a Translating Spike Inlet Employing a Steep-Lip Cowl. NACA RM E54G29, 1954.
2. Moeckel, W. E., and Evans, P. J., Jr.: Preliminary Investigation of Use of Conical Flow Separation for Efficient Supersonic Diffusion. NACA RM E51J08, 1951.
3. Connors, James F., and Woollett, Richard R.: Characteristics of Flow about Axially Symmetric Isentropic Spikes for Nose Inlets at Mach Number 3.85. NACA RM E54F08, 1954.
4. Connors, James F., and Meyer, Rudolph C.: Performance Characteristics of Axisymmetric Two-Cone and Isentropic Nose Inlets at Mach Number 1.90. NACA RM E55F29, 1955.
5. Hunczak, Henry R.: Pressure Recovery and Mass-Flow Performance of Four Annular Nose Inlets Operating in Mach Number Region of 3.1 and Reynolds Number Range of Approximately  $0.45 \times 10^6$  to  $2.20 \times 10^6$ . NACA RM E54A07, 1954.

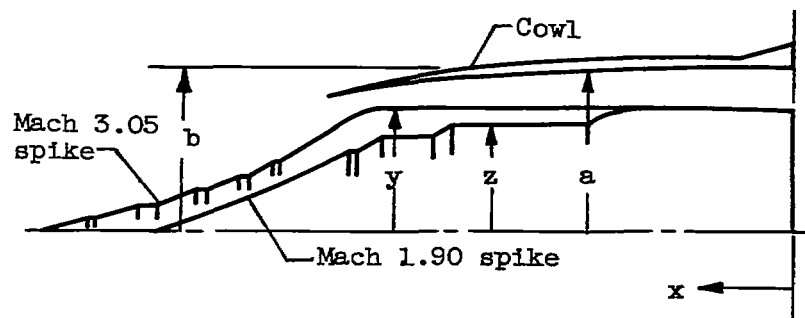
TABLE I. - DIMENSIONS OF SURVEY SPIKE CONFIGURATIONS  
 [30° Survey spike formed by adding rings indicated by solid areas.]



| Point on<br>envelope contour | Coordinate dimensions |                    |
|------------------------------|-----------------------|--------------------|
|                              | x                     | y (Diam.)          |
| a                            | 0.000                 | <sup>a</sup> 0.000 |
| b                            | .408                  | .125               |
| c                            | 1.350                 | .375               |
| d                            | 3.056                 | .875               |
| e                            | 4.520                 | 1.375              |
| f                            | 5.642                 | 1.875              |
| g                            | 6.540                 | 2.375              |
| h                            | 7.272                 | 2.875              |
| i                            | 7.880                 | 3.375              |
| j                            | 8.274                 | <sup>a</sup> 3.796 |
| k                            | 9.304                 | 4.970              |

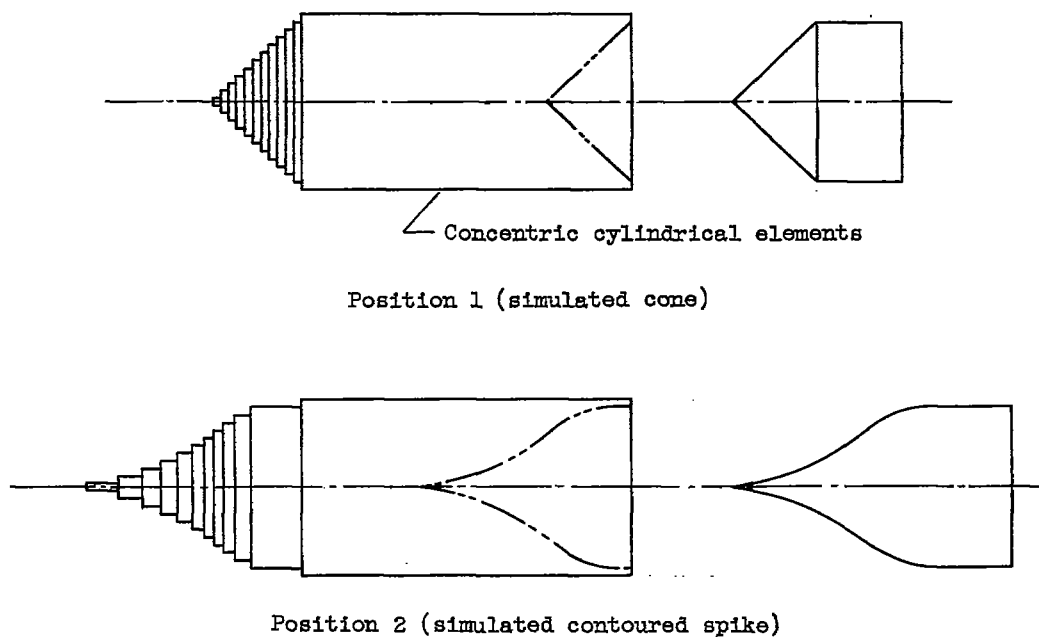
<sup>a</sup>Followed by straight taper section.

TABLE II. - DIMENSIONS OF VARIABLE-GEOMETRY INLET

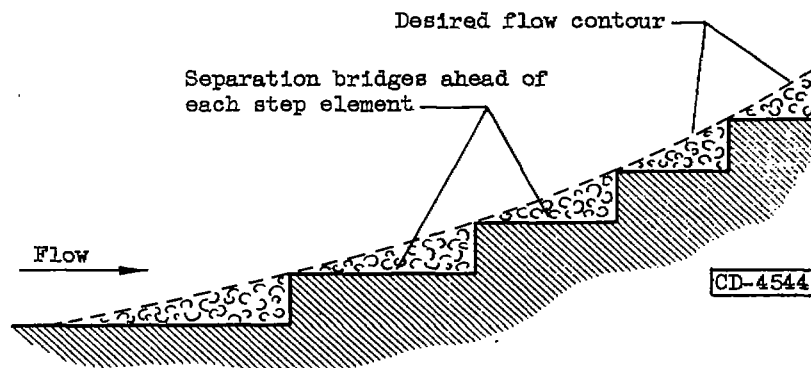


| Mach 3.05 spike |                    | Mach 1.90 spike |                    | Cowl  |                    |                    |
|-----------------|--------------------|-----------------|--------------------|-------|--------------------|--------------------|
| x               | y (Rad.)           | x               | z (Rad.)           | x     | a                  | b                  |
| 0.000           | 1.320              | 0.000           | 1.320              | 0.000 | <sup>a</sup> 1.800 | <sup>b</sup> 2.074 |
| .360            | 1.332              | .320            | 1.332              | .600  | <sup>a</sup> 1.800 | <sup>a</sup> 1.900 |
| .667            | <sup>a</sup> 1.340 | .670            | <sup>a</sup> 1.340 | 1.390 | 1.800              | <sup>a</sup> 1.900 |
| 4.340           | 1.340              | 1.570           | 1.340              | 1.890 | 1.795              | 1.900              |
| 4.440           | 1.330              | 1.670           | 1.339              | 2.390 | 1.777              | 1.888              |
| 4.540           | 1.309              | 1.820           | 1.324              | 2.690 | 1.760              | 1.888              |
| 4.640           | 1.262              | 1.970           | 1.273              | 2.890 | <sup>b</sup> 1.760 | 1.850              |
| 4.740           | 1.198              | 2.100           | 1.189              | 3.390 | 1.760              | 1.799              |
| 4.890           | 1.088              | 3.502           | 1.189              | 3.890 | 1.657              | 1.732              |
| 5.040           | .983               | 3.001           | 1.115              | 4.140 | 1.633              | 1.688              |
| 5.290           | .831               | 3.700           | 1.041              | 4.390 | 1.592              | 1.629              |
| 5.437           | .744               | 4.270           | 1.041              | 4.640 | 1.528              | 1.550              |
| 5.459           | .744               | 4.370           | .967               | 4.888 | 1.450              | 1.455              |
| 5.590           | .667               | 4.488           | .891               |       |                    |                    |
| 5.723           | .595               | 4.570           | .891               |       |                    |                    |
| 5.816           | .595               | 4.770           | .773               |       |                    |                    |
| 5.940           | .532               | 5.070           | .605               |       |                    |                    |
| 6.114           | .446               | 5.320           | .476               |       |                    |                    |
| 6.260           | .446               | 5.470           | .405               |       |                    |                    |
| 6.440           | .371               | 5.608           | <sup>b</sup> .352  |       |                    |                    |
| 6.627           | <sup>a</sup> .298  | 6.570           | .000               |       |                    |                    |
| 6.796           | <sup>b</sup> .298  |                 |                    |       |                    |                    |
| 7.212           | <sup>a</sup> .149  |                 |                    |       |                    |                    |
| 7.359           | <sup>b</sup> .149  |                 |                    |       |                    |                    |
| 7.790           | .000               |                 |                    |       |                    |                    |

<sup>a</sup>Followed by cylindrical section.<sup>b</sup>Followed by straight taper section.



(a) Variable-geometry centerbody (telescoping spike) scheme.

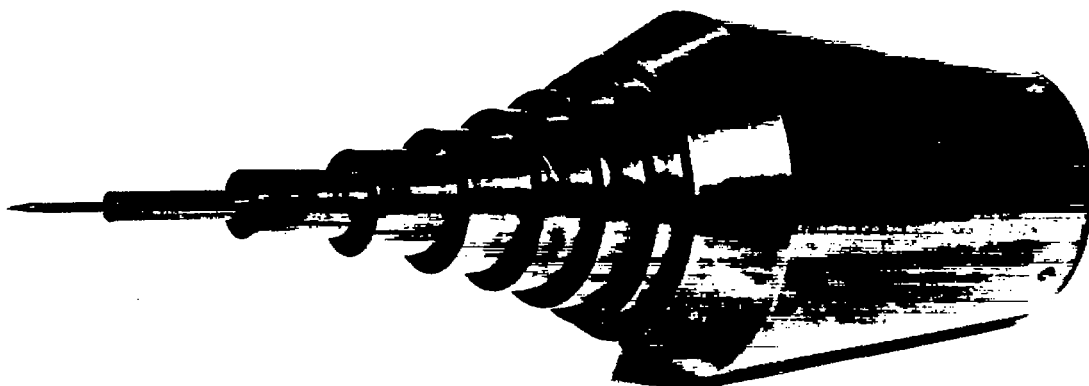


(b) Flow pattern along surface discontinuities.

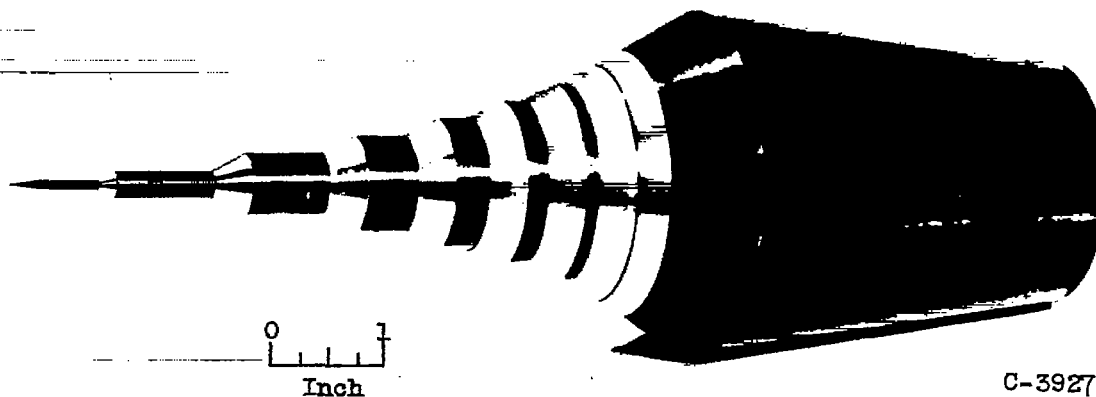
Figure 1. - Schematic sketches of proposed axisymmetric variable-geometry technique.



(a) Smooth-contour spike.



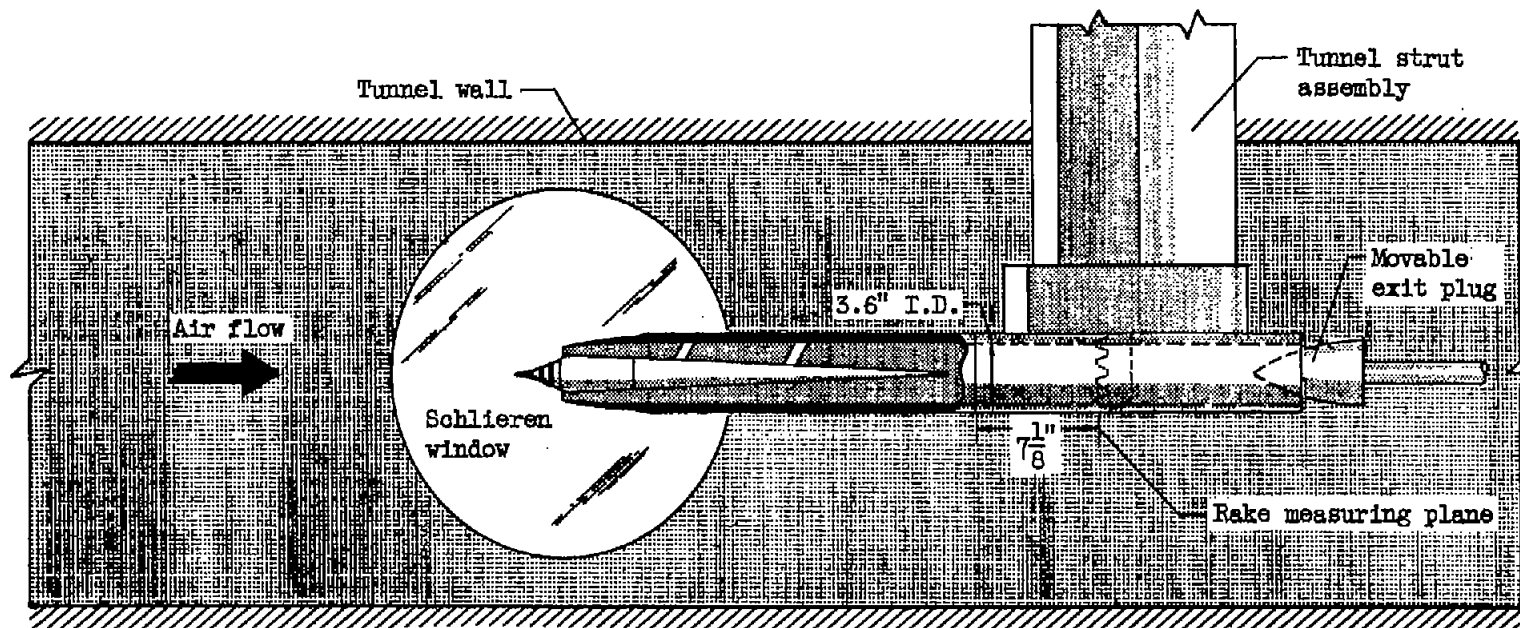
(b) 90° Stepped spike.



(c) 30° Stepped spike.

C-39273

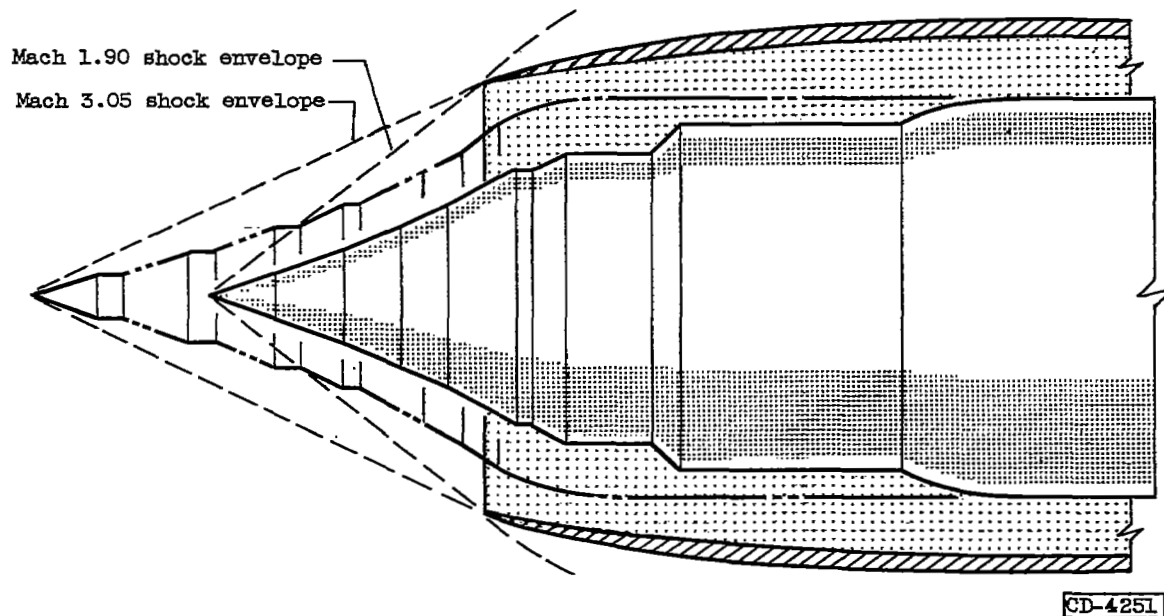
Figure 2. - Experimental survey spikes for study of flow over surface discontinuities at free-stream Mach number of 3.85.



CD-4250

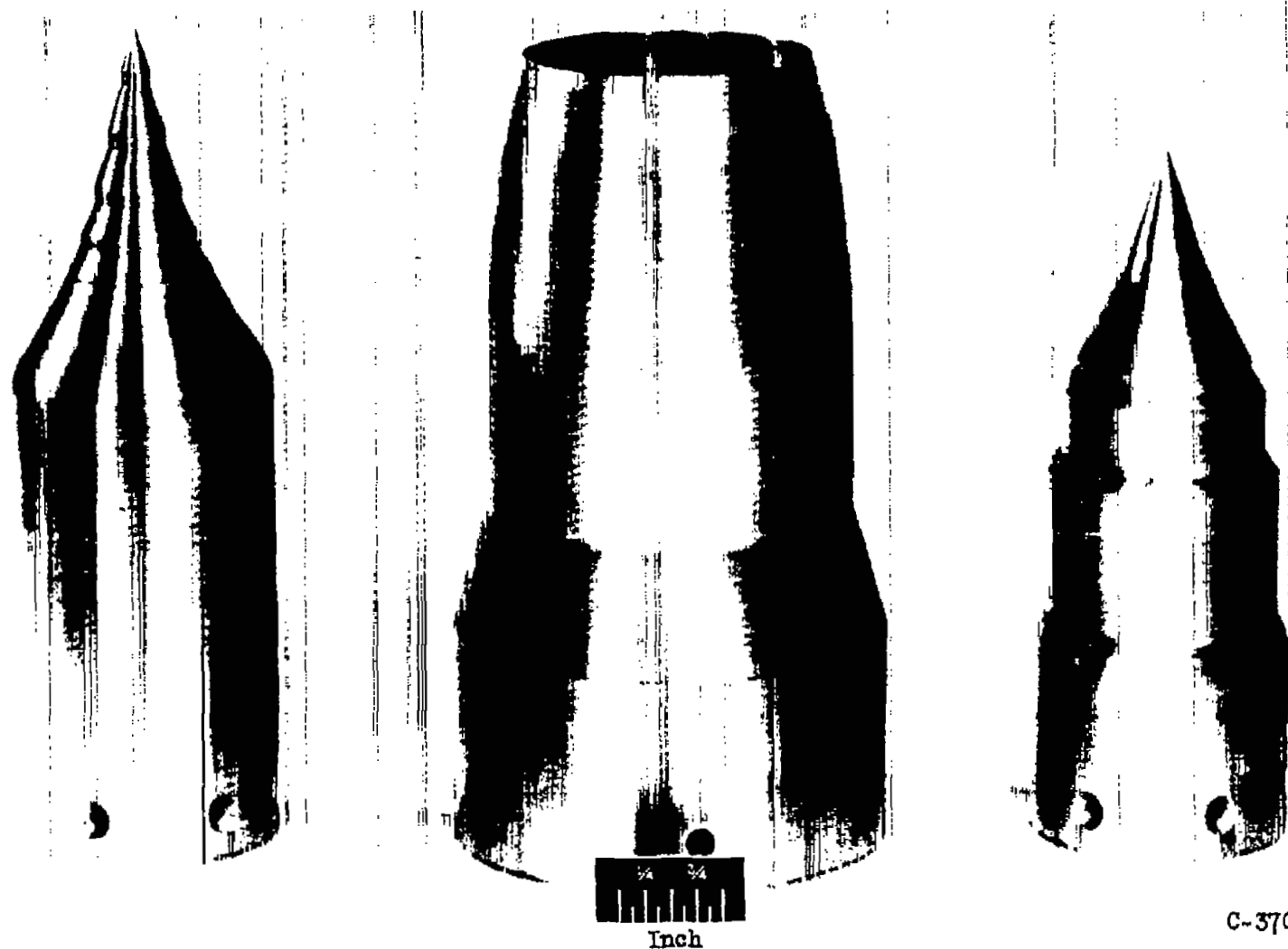
(a) Tunnel installation.

Figure 3. - Experimental apparatus for study of variable-geometry inlet.



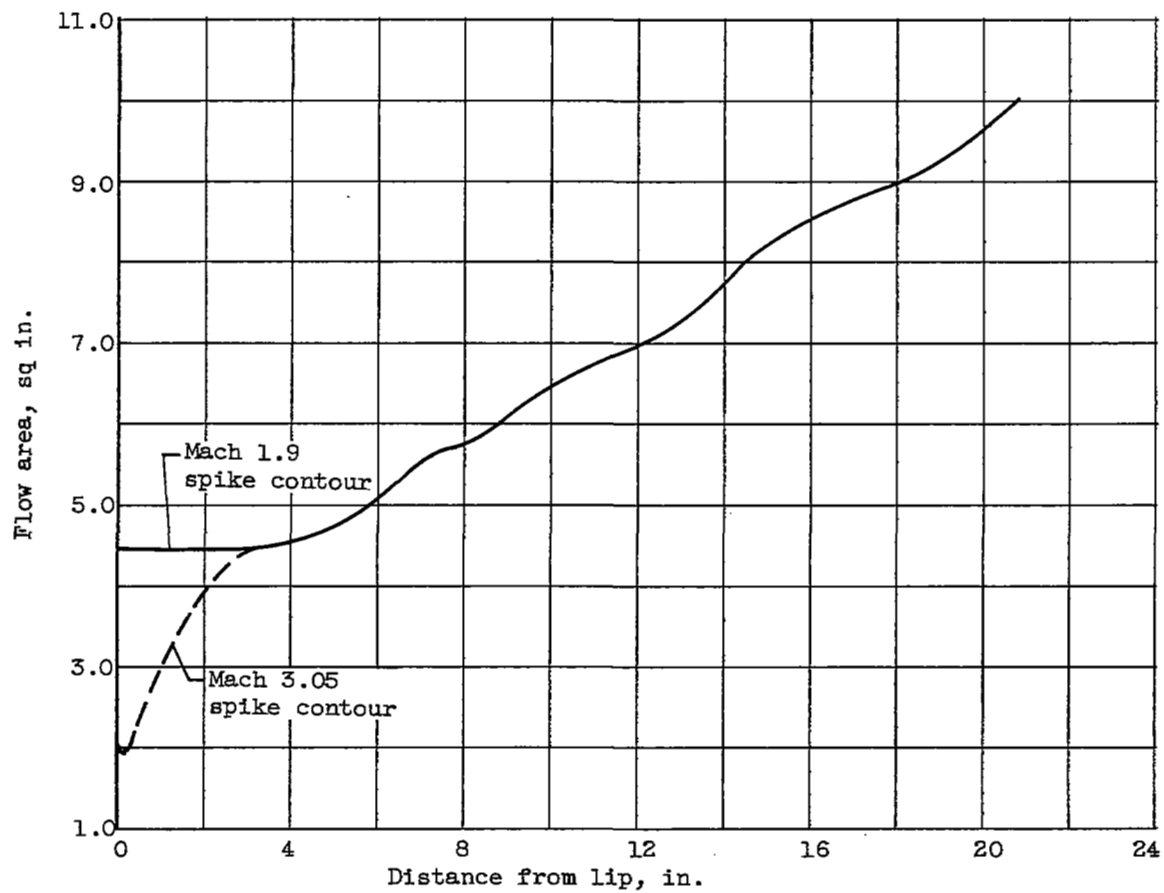
(b) Variable-geometry inlet (telescoping spike).

Figure 3. - Continued. Experimental apparatus for study of variable-geometry inlet.



(c) Cowl and spikes.

Figure 3. - Continued. Experimental apparatus for study of variable-geometry inlet.



(d) Internal duct area variation based on envelope contours.

Figure 3. - Concluded. Experimental apparatus for study of variable-geometry inlet.



(a)  $90^\circ$  Stepped spike.



(b)  $30^\circ$  Stepped spike.

Figure 4. - Flow patterns obtained with stepped spikes. Free-stream Mach number, 3.85.

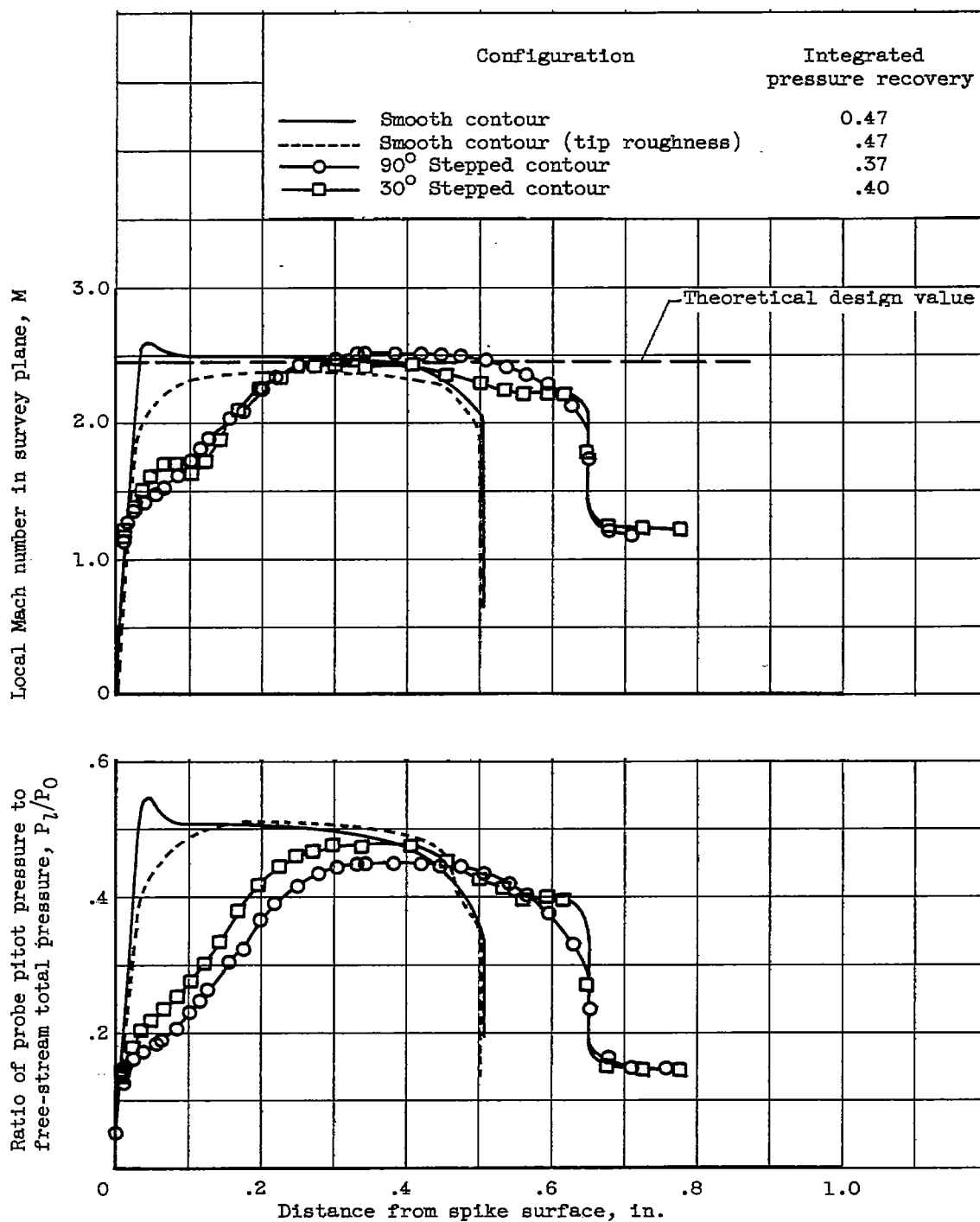


Figure 5. - Mach number and pitot-pressure profiles for stepped and smooth spikes. Free-stream Mach number,  $M_0$ , 3.85.

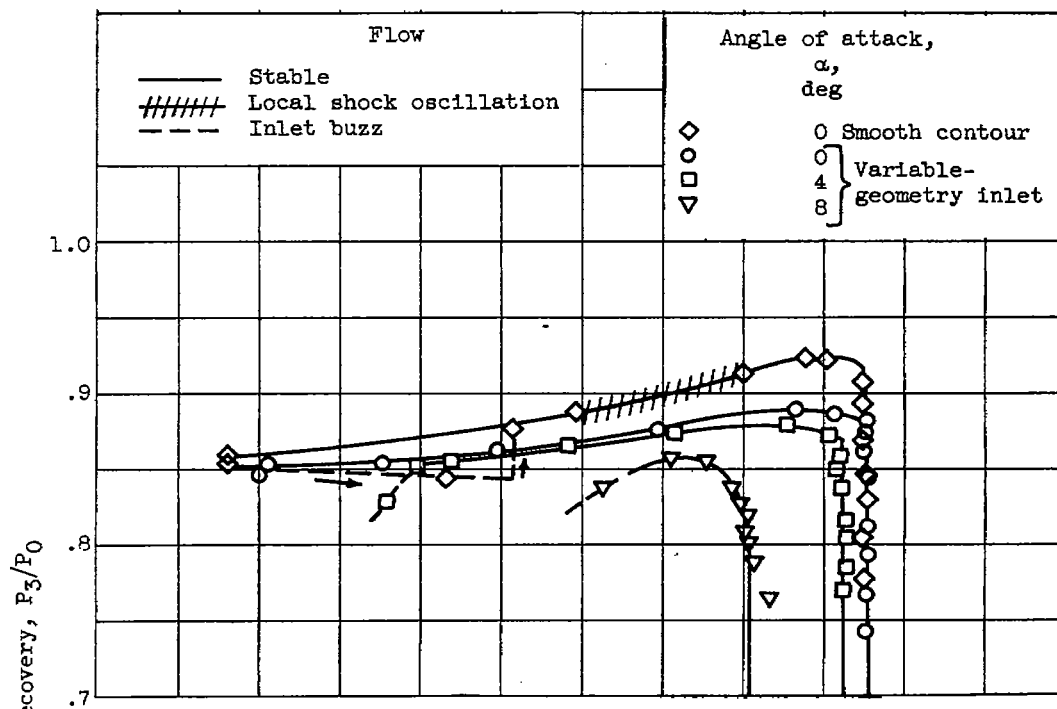
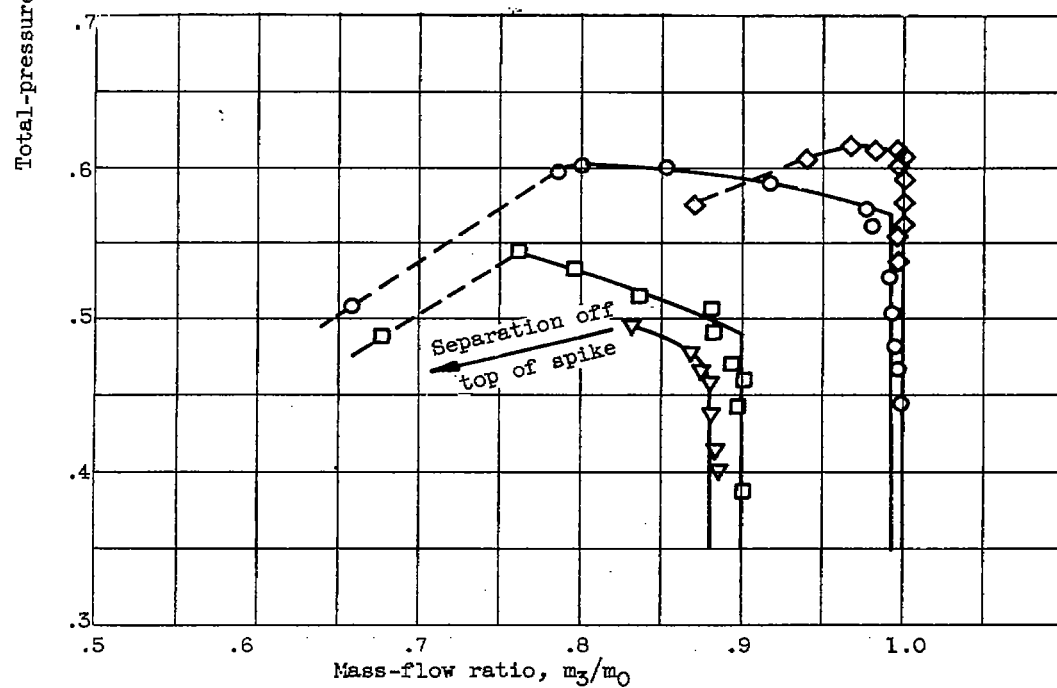
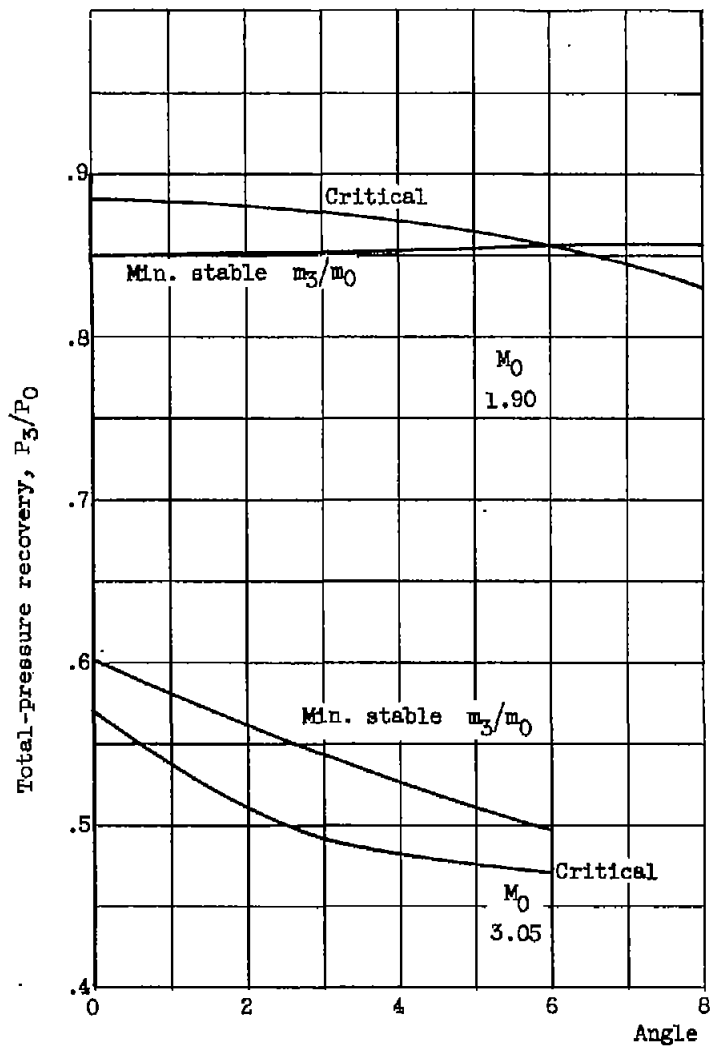
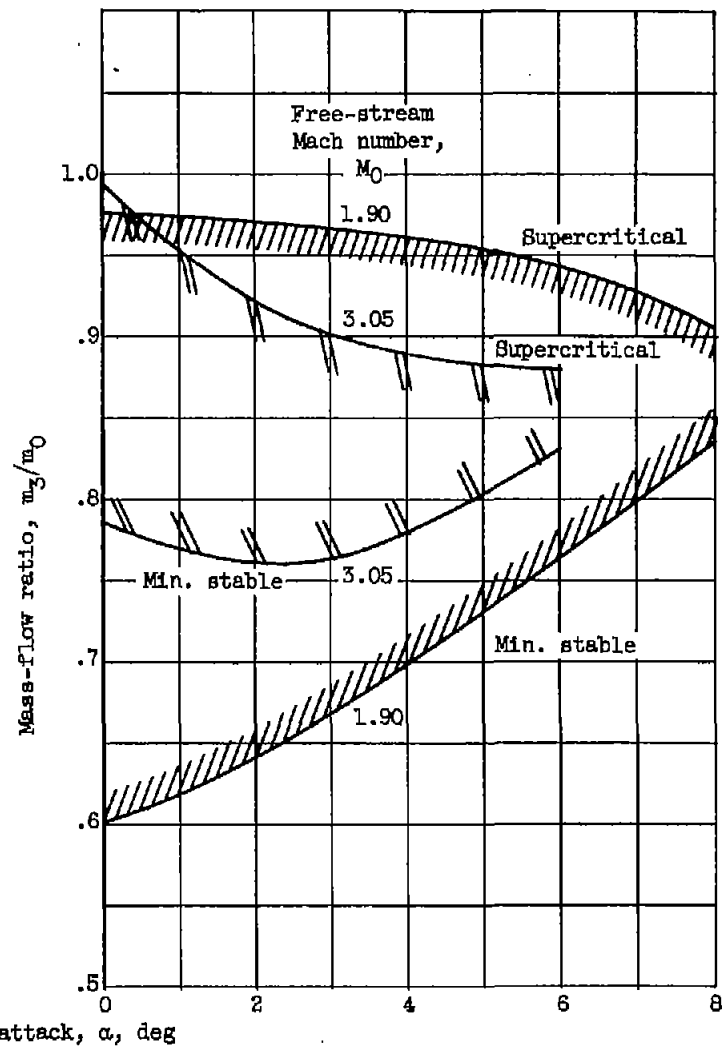
(a) Free-stream Mach number,  $M_0$ , 1.90.(b) Free-stream Mach number,  $M_0$ , 3.05.

Figure 6. - Performance characteristics of variable-geometry inlet.

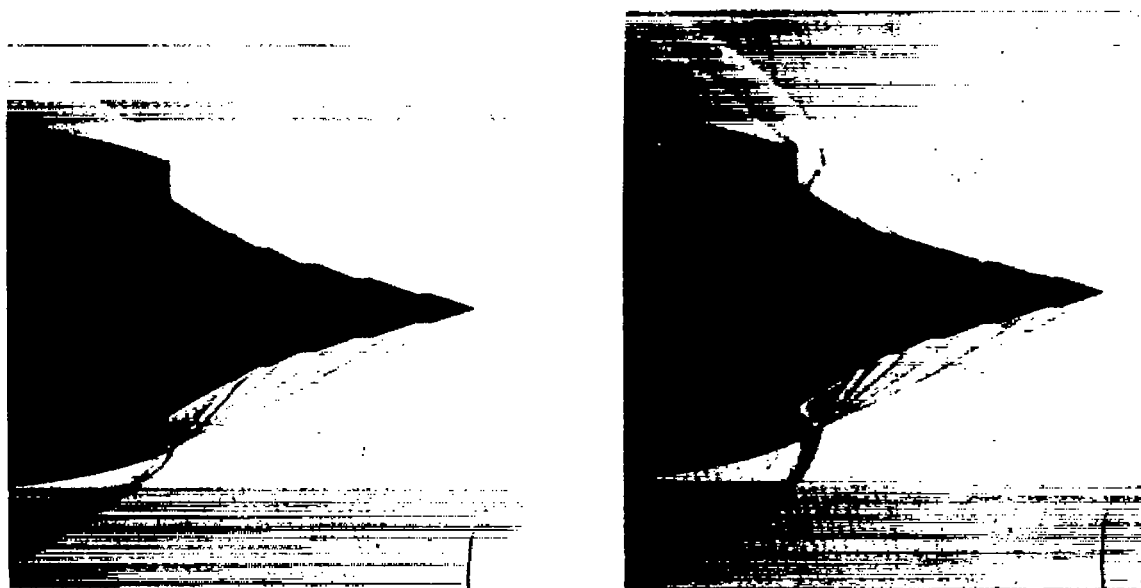


(a) Total-pressure recovery.



(b) Mass-flow ratio.

Figure 7. - Effect of angle of attack on performance of variable-geometry inlet.

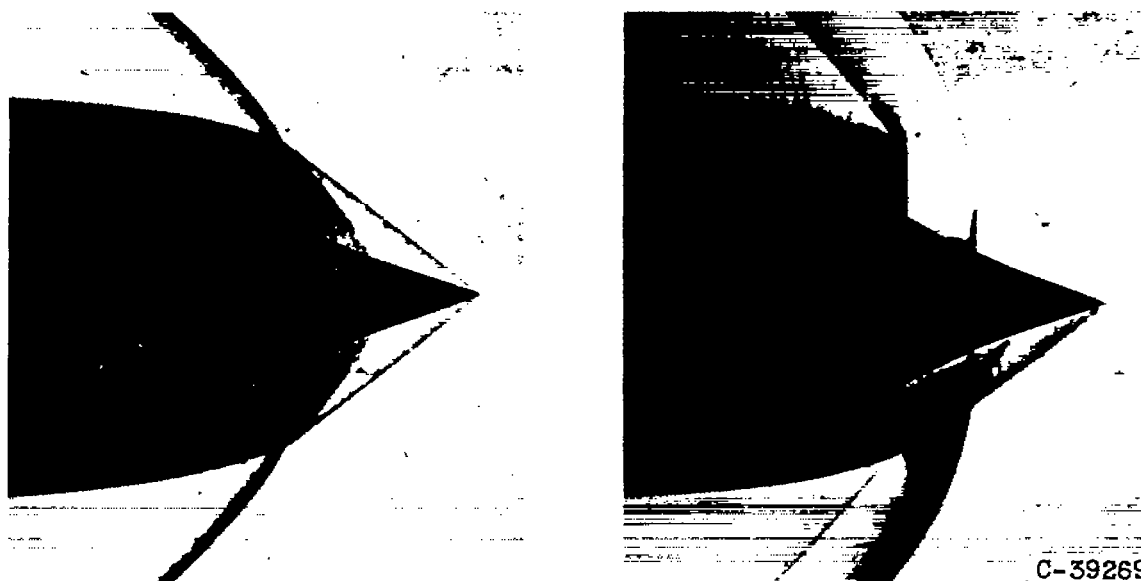


Supercritical

Mass-flow ratio

Minimum stable

(a) Free-stream Mach number, 3.05; zero angle of attack.



Supercritical

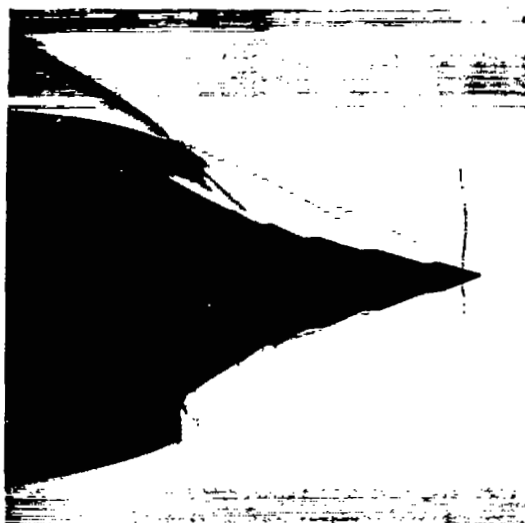
Mass-flow ratio

Minimum stable

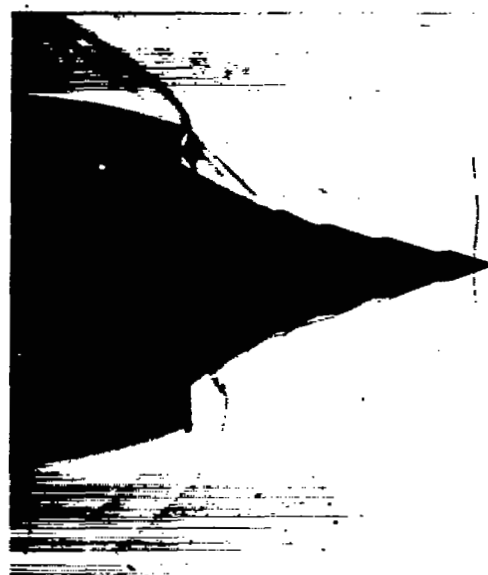
C-39269

(b) Free-stream Mach number, 1.90; zero angle of attack.

Figure 8. - Flow patterns for variable-geometry inlet at various angles of attack.



Supercritical



Minimum stable

Mass-flow ratio

(c) Free-stream Mach number, 3.05; angle of attack,  $3^\circ$ .

Supercritical



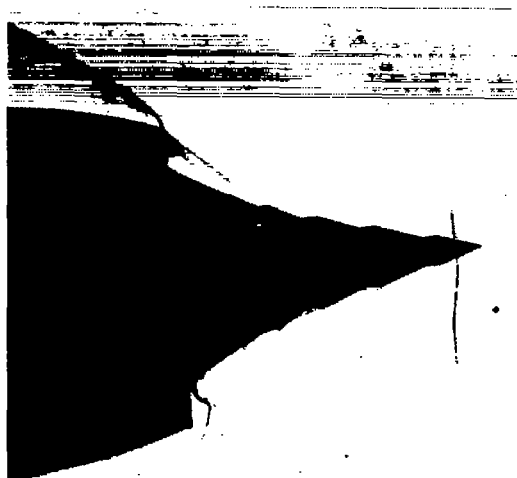
Minimum stable

Mass-flow ratio

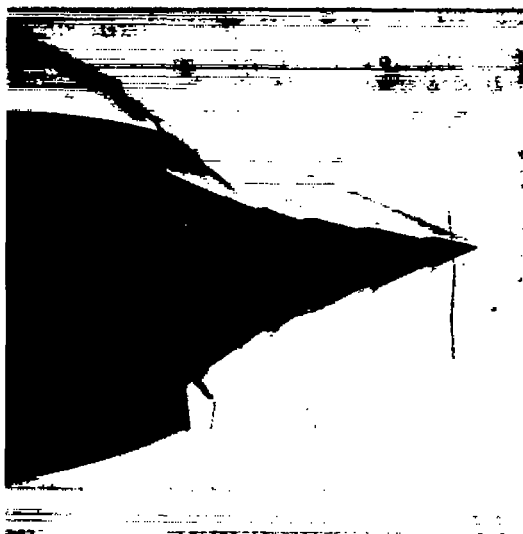
(d) Free-stream Mach number, 1.90; angle of attack,  $4^\circ$ .

Figure 8. - Continued. Flow patterns for variable-geometry inlet at various angles of attack.

C-39270



Supercritical



Minimum stable with attached flow



Separation off spike (steady pattern)

C-39271

Mass-flow ratio

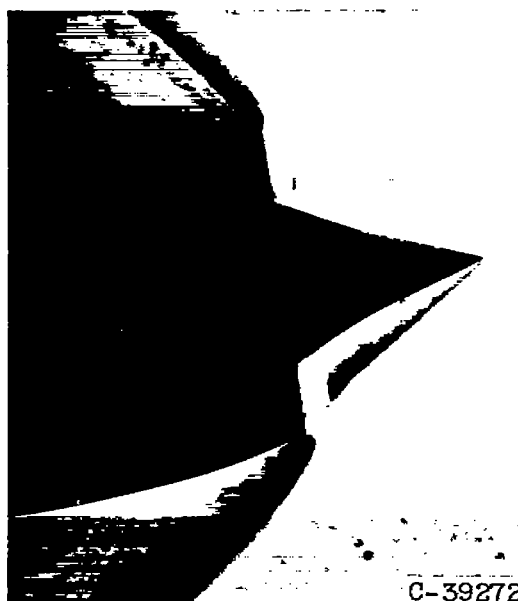
(e) Free-stream Mach number, 3.05; angle of attack,  $6^\circ$ .

Figure 8. - Continued. Flow patterns for variable-geometry inlet at various angles of attack.

3756



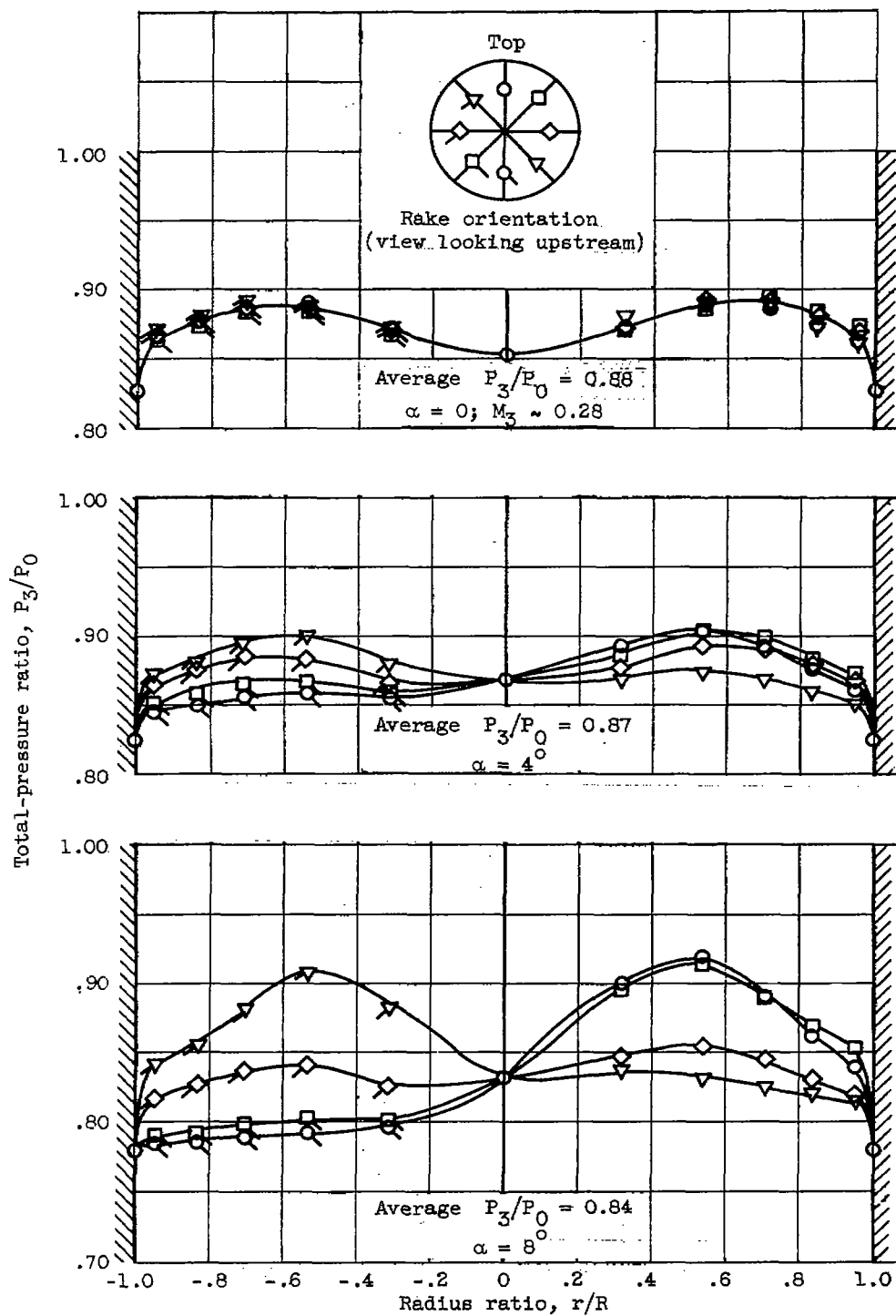
Supercritical



C-39272

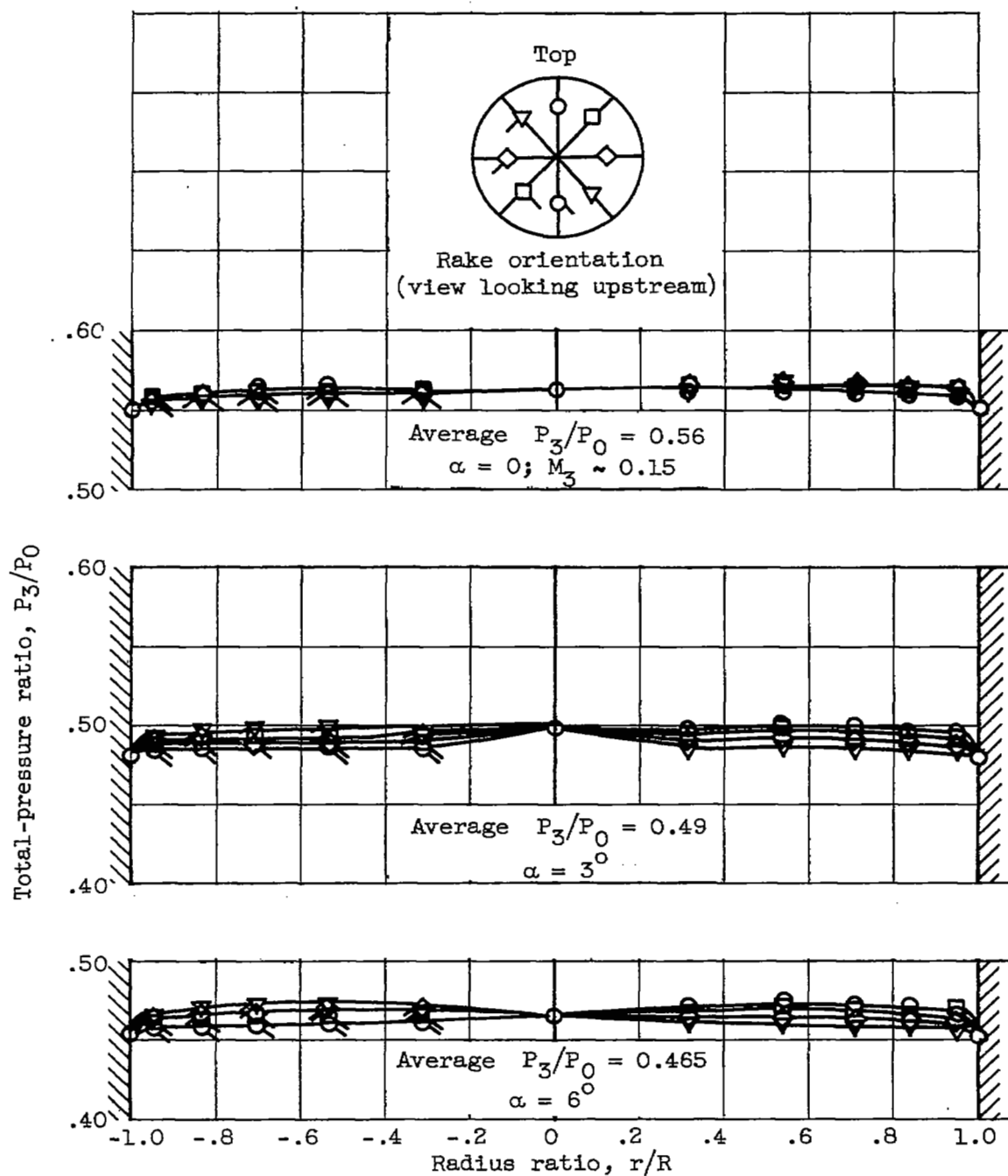
Minimum stable  
Mass-flow ratio(f) Free-stream Mach number, 1.90; angle of attack,  $8^\circ$ .

Figure 8. - Concluded. Flow patterns for variable-geometry inlet at various angles of attack.



(a) Free-stream Mach number, 1.90.

Figure 9. - Total-pressure profiles across diffuser exit at critical operation.



(b) Free-stream Mach number, 3.05.

Figure 9. - Concluded. Total-pressure profiles across diffuser exit at critical operation.



LANGLEY RESEARCH CENTER

3 1176 01345 8063